Optical influence of oil droplets on cone photoreceptor sensitivity

David Wilby and Nicholas W. Roberts

Ecology of Vision Laboratory, School of Biological Sciences, Life Sciences Building, Tyndall Avenue, University of Bristol, Bristol. BS8 1TQ. United Kingdom.

Corresponding author: Dr. David Wilby
+44 117 95 41350 david.wilby@bristol.ac.uk

Keywords: oil droplets, ellipsoid, optics, cone, photoreceptor, vision.

Summary statement: The internal structure of photoreceptor cells influences their sensitivity to light. We have used optical simulations to study how both oil droplets and ellipsoids in cone photoreceptors can impact sensitivity.

Abstract

Oil droplets are spherical organelles found in the cone photoreceptors of vertebrates. They are generally assumed to focus incident light into the outer segment, and thereby improve light catch because of the droplets' spherical lens-like shape. However, using full-wave optical simulations of physiologically realistic cone photoreceptors from birds, frogs and turtles we find that pigmented oil droplets actually drastically reduce the transmission of light into the outer segment integrated across the full visible wavelength range of each species. Only transparent oil droplets improve light catch into the outer segments, and any enhancement is critically dependent on the refractive index, diameter of the oil droplet, and diameter and length of the outer segment. Furthermore, oil droplets are not the only optical elements found in cone inner segments. The ellipsoid, a dense aggregation of mitochondria situated immediately prior to the oil droplet, mitigates the loss of light at oil droplet surface. We describe a framework for integrating these optical phenomena into simple models of receptor sensitivity and the relevance of these observations to evolutionary appearance and loss of oil droplets is discussed.

Introduction

The cone photoreceptors of around half of the orders of vertebrates contain spherical structures composed of lipids and carotenoid pigment, known as oil droplets (Walls, 1942; Jacobs and Rowe, 2004). Oil droplets are situated immediately prior to the light-sensitive outer segment in the light path, and their role is to influence the light that reaches it. Many oil droplets contain mixtures of carotenoid pigment (Johnston and Hudson, 1976; Toomey et al., 2015) and have been predominantly studied for their spectral filtering properties (eg Partridge, 1989; Hart, 2001) and their influence on tuning the spectral sensitivity of colour vision, thereby improving colour discrimination and colour constancy (Vorobyev, 2003). However, the oil droplets of ultra-violet and violet sensitive cones are transparent across the visible spectrum (Bowmaker et al., 1997), containing no pigment. Further to this, numerous species (Fig. 1) only have transparent oil droplets in all of their cone types. This widespread presence of transparency therefore indicates that oil droplets must serve a purpose other than just spectral filtering (Walls, 1942; Hart, 2001).

Oil droplets have a relatively high refractive index, spherical shape and are typically wider than the outer segment (Ives et al., 1983, Young and Martin, 1984, Wilby et al. 2015). Being able to enlarge the area of light capture without increasing the size of the outer segment, should in theory improve the signal-to-noise ratio and reduce energetic cost (Ives et al., 1983, Young and Martin, 1984, Stavenga and Wilts, 2014). Nevertheless, the extent to which oil droplets improve light capture is still unclear. Prior efforts have proposed that oil droplets gather more light into the outer segment (Govardovskii et al., 1981; Ives et al., 1983; Young and Martin, 1984; Stavenga and Wilts, 2014). This might not however be the case for all oil droplets, with a recent study discovering that the pigmented droplets in simulations of cone photoreceptors in the chicken (*Gallus gallus domesticus*) reduced transmission of light into the outer segment for the regions of the spectrum to which the visual pigments were sensitive (Wilby et al., 2015). Only the transparent oil droplet of the violet cone increased light transmission into the outer segment by approximately 50%.

This raises several questions: what properties of oil droplets influence light catch? How do oil droplets perform relative to the 'ideal' light-coupling scenario in

which all incident light within the area of the oil droplet is focused into the outer segment?

In this study, we use numerical optical calculations informed by morphological and optical measurements to investigate the influence oil droplets have on optical power in the outer segment. We include the optics of the outer segment, which itself acts as a waveguide to confine light to the regions of the retina containing the light sensitive pigment. Finally we examine the optical role of the ellipsoid in conjunction with the oil droplet in the concentration of light into the outer segment.

Materials and Methods

Optical simulations

Calculations were performed with the freely available finite-difference time-domain simulation software, MEEP (MPI version 1.2; Oskooi et al. 2010) using the computational facilities of the Advanced Computing Research Centre, University of Bristol. Simulations took advantage of the rotational symmetry of the models about the *z*-axis and computations were performed in cylindrical polar coordinates for a thin wedge of the model (see supplementary information fig. S1). Carotenoid absorption spectra along with refractive index measurements were used to model the dielectric function of the oil droplets as previously described (Wilby et al., 2015).

For models of oil droplets based on the three species in this study (chicken, *Gallus gallus domesticus*; red-eared slider, *Trachemys scripta elegans*; African clawed frog, *Xenopus laevis*), calculations were performed for specific oil droplet and outer segment dimensions. Dimensions and refractive indices were taken from the literature and are summarised in supplementary table S2. For simplicity, a wavelength-invariant value of refractive index of 1.45 was used for the outer segment as measured previously (Wilby et al., 2015). The refractive index change of the lipid membrane across the visible spectrum is <0.01 (Roberts et al., 2009) and the visual pigment has minimal influence on the refractive index (Stavenga and van Barneveld, 1975). Analyses of the sensitivity of the models to the refractive index of the outer segment demonstrated that a value of 1.45 is a conservative choice. The surrounding

media which was given the refractive index 1.35 as calculated by Enoch and Tobey (1978). Simulations that incorporated the ellipsoid, modelled it as a cylinder preceding the oil droplet and surrounding its front hemisphere, similarly to Wilby et al. (2015). Ellipsoids were equal in radius to the oil droplet, had a refractive index of 1.43 and were 3.5 μm long. Full details of all simulation parameters are given in supplementary table S2.

Following Ives et al., (1983) we define the volume-averaged enhancement factor, *D*, as the ratio of the integral of $\boldsymbol{E}.\boldsymbol{E}^*$ (as a proxy for light intensity), within the outer segment in the presence of an oil droplet (OD) to the integrated electric field intensity in the absence of the oil droplet (NOD)

$$D(\lambda) = \frac{[\iint \boldsymbol{E}(\lambda).\boldsymbol{E}(\lambda)^* \mathrm{d}\phi \mathrm{d}r]_{\mathrm{OD}}}{[\iint \boldsymbol{E}(\lambda).\boldsymbol{E}(\lambda)^* \mathrm{d}\phi \mathrm{d}r]_{\mathrm{NOD}}}. \quad (1)$$

Integrals were performed numerically in cylindrical polar coordinates over the volume of the outer segment (which effectively reduces to an area under cylindrical symmetry). The electric field vector is composed of components [E_r E_ϕ E_z] along the radial, polar and *z* (propagation) axes respectively. The complex conjugate is indicated by *.

Additionally, we define an enhancement as predicted using the geometry alone, as the ratio of the cross-sectional areas of the oil droplet and the outer segment, which reduces to

$$D_G = \frac{d_{\mathrm{OD}}^2}{d_{\mathrm{OS}}^2} \quad (2)$$

where d_{OD} and d_{OS} are the diameter of the oil droplet and the outer segment closest to the oil droplet respectively. This is analogous to the use of the oil droplet diameter as the photoreceptor diameter in typical photoreceptor sensitivity calculations (eg Land 1981; Warrant and Nilsson, 1998). We also define the fraction, *F*, of light arriving within the cross-sectional area of the oil droplet that upon focusing arrives in the outer segment given by

$$F = \frac{D}{D_G}, \quad (3)$$

which can be incorporated into existing models of photoreceptor sensitivity (eg Land 1981; Warrant and Nilsson, 1998) as a multiplicative factor which accounts for losses and gains due to optical phenomena (Olsson et al., 2017).

Measurement of oil droplet refractive index

X. laevis adults were culled by an overdose of anaesthetic (MS222) and destruction of the central nervous system according to the ethical guidelines of the University of Bristol. Eyes were enucleated from 2 animals, hemisected and the retina removed. Pieces of retina approximately 2x2 mm^2 were separated by repeated pipetting in deionized water and centrifuged at 14 krpm for 2 mins.

For *X. laevis* oil droplets, refractive indices were measured for this study using a commercial digital holographic microscope (DHM; T1000; LyncéeTec, Lausanne, Switzerland). Measurements were made at free-space wavelengths of 445, 488, 515 and 640 nm. The refractive index measurement method of Schürmann et al. (2015) was implemented using a combination of proprietary DHM software, Koala (LyncéeTec, Lausanne, Switzerland) and bespoke code written in Matlab (v8.3; Mathworks, Natick, MA, USA).

The two-term Cauchy relation

$$n(\lambda) = B + \frac{C}{\lambda^2}, \qquad (4)$$

where n is the refractive index as a function of free-space wavelength, λ, and B and C are the Cauchy coefficients, was fitted to the discrete measurements to calculate wavelength dependence of the refractive index of *Xenopus* oil droplets. The Cauchy relation, in comparison to the more physically descriptive Sellmeier equation, is accurate in the wavelength range used here for normally dispersive materials and is somewhat simpler (Born and Wolf 1999; Leertouwer et al. 2011).

Oil droplet refractive indices and absorbance spectra (as a function of wavelength) for *G. gallus* were taken from Wilby et al. (2015); for *T. scripta elegans* from Ives et al. (1983), Liebman and Granda (1971) and Strother (1963).

Results

First, we present the results of how variation in the geometry and refractive index of the oil droplets affect the light catch in model outer segments. We then use the models of cone photoreceptors from the three species of *G. gallus domesticus*, *T. scripta elegans* and *X. laevis* that are based on geometrical and optical measurements of real photoreceptor cells to investigate how oil droplet pigments affect optical enhancement and absorption. Lastly, we show how the ellipsoid of chicken photoreceptors plays a role in light catch enhancement.

Higher oil droplet refractive index decreases light catch

In simulations of transparent oil droplets before cylindrical, conical and truncated-conical outer segments, the enhancement factor decreased as the refractive index of the oil droplet, $n_{OD,}$ increased (fig. 2). Moreover, the enhancement factors do not reach the ideal predicted using receptor geometry, D_G. In cylindrical outer segments, similar to chicken cones (d_{OD}=3 μm; d_{OS}=1.5 μm; l_{OS}=30 μm, Wilby et al., 2015) D_G is 4 but calculated enhancement factors vary between 0.6 – 1.7 with the lowest values occurring for higher n_{OD} and longer wavelength (fig. 2A). For the conical outer segment model, similar to amphibian cones (d_{OD}=3.1 μm; d_{OS}=2.25 μm; l_{OS}=12 μm, Röhlich and Szél, 2000) enhancement factors are predominantly >1 but again do not reach the D_G of 1.90 (fig. 2B). Similarly in the truncated cone model, similar to turtle cones (d_{OD}=2.5 μm; d_{OS}=1.5-0.5 μm; l_{OS}=10 μm, Ives et al. 1983), enhancement factors are >1 but do not reach the D_G of 2.78 (fig. 2C).

Oil droplets enhance light catch more for shorter outer segments

We created sets of simulations with varying l_{OS} for cylindrical outer segments with d_{OS}=1.5 μm and oil droplets of the same or double the diameter. In both cases, enhancement factors were larger for shorter outer segments (fig. 3). This effect, however, is relatively small over the range of outer segment lengths found in nature, since the values of l_{OS} used here were 10, 20 and 30 μm. For oil droplets of the same diameter as the outer segment (fig. 3A), enhancement factors were $<D_G = 1$. For oil droplets double the diameter (fig. 3B), enhancement factors never approached the D_G of 4.

Greater enhancement for larger oil droplets and wider outer segments

In sets of simulations for constant dimensions of the outer segment but increasingly large oil droplets, enhancement was greater for larger oil droplets (fig. 4). For d_{OD}=d_{OS}, enhancement factors approached the D_G of 1. For d_{OS}=3 μm enhancement was very close to 1 and even slightly greater for some wavelengths; the only scenario tested here in which the simulated enhancement factor exceeded the geometrically predicted value. For larger oil droplets, enhancement was increased above 1, but did not approach the D_G of 4. The simulation sets presented in fig. 4 illustrate examples for which the geometrically predicted values are the same but have differing dimensions. For instance, the geometrically predicted values for the solid lines in fig. 4A and B have an equal value of 4 but have largely differing enhancement factor curves with the greater values occurring for larger d_{OS} and d_{OD}.

Refractive index of *Xenopus laevis* oil droplets

In order to create an optical simulation for the cones of *X. laevis,* which has only transparent oil droplets, we first had to measure the oil droplet refractive index as a function of wavelength. The refractive index measurement method resulted in large variance, though normally distributed (fig. 5). The two-term Cauchy relation (eqn. 4) was fit to these measurements to calculate the refractive index of the oil droplets as a function of wavelength. The Cauchy coefficients for the fit were B=1.4311 and C=3.8×10^3 nm^2. We also found no evidence of more than one population of oil droplets with respect to their refractive index; indicating that the oil droplets in different classes of cone in *Xenopus* share similar optical properties (see supplementary fig. S2). As is typical of non-absorbing materials, the dispersion is weak across the 350-700 nm wavelength range (Born and Wolf, 1999).

Pigmented droplets reduce light catch for relevant wavelengths

Enhancement factors were calculated for oil droplet models with refractive indices, dimensions and absorption spectra for cone photoreceptors of *X. laevis, G. gallus* and *T. scripta elegans* (fig. 6A-C). Enhancement factors for the pigmented droplets of chicken and turtles generally reflected those for transparent droplets in regions of the spectrum for which there was low absorption of light in the oil droplet. Predictably, low values of enhancement were seen where absorption was strong (fig. 6B,C,E,F). The transparent droplet of *X. laevis* has an enhancement factor >1 covering the entire

spectrum, universally increasing light catch (fig. 6D). However, for regions of the spectrum for which the visual pigments are sensitive, and particularly at the wavelength of peak visual pigment sensitivity (λ_{max}) of the cones, pigmented droplets mostly reduce light catch and hence cone sensitivity (fig. 6E,F,H,I). Oil droplets in chicken photoreceptors are all predicted to have enhancement factors <1 (ie reduce light catch, fig. 6E,H). Those in turtle photoreceptors, while having enhancement factors >1 for longer wavelengths, have values <1 at the λ_{max} of all three cone types (fig. 6I).

Ellipsoids improve enhancement

Currently *G. gallus* is the only species for which all the requisite optical and structural measurements of the ellipsoid are available (Wilby et al. 2015). The modelling data demonstrated that in this species, the ellipsoid has a substantial effect on the optics and the addition of the ellipsoid in the VS, SWS and MWS cones increased the enhancement factor (fig. 7A). The greatest enhancement was seen for the VS cone, for which the enhancement is approximately doubled on addition of the ellipsoid. Enhancement also becomes almost entirely >1 for wavelengths to which the VS cone is sensitive (fig. 7B).

It is clear that the ellipsoid increases the enhancement within VS, SWS and MWS chicken cones, particularly the transparent VS cone and it is logical to assume that similar optical effects take place for the ellipsoids of cones in other species with both transparent and pigmented oil droplets. This leads to a conclusion that the enhancements shown in fig. 6 for *X. laevis* and *T. scripta elegans* are likely to underestimate real enhancement similarly to the case for the chicken.

Discussion

The extent of enhancement in light catch provided by an oil droplet is profoundly variable across different types of cone as well as across the visible spectrum. We have shown that several factors combine to influence the light coupling into the outer segment. These include, but are not limited to: the oil droplet refractive index; dimensions of the oil droplet and outer segment; and the presence and refractive index of the ellipsoid, which are discussed below.

Cone structure and oil droplet refractive index

We have calculated the change in light intensity in the outer segment due to the optical influence of transparent oil droplets in order to investigate the effects of cone refractive index and geometry on the passage of light and hence sensitivity. To summarise the combined effects of these changes:

1. An increase in refractive index compromises the ability of the oil droplet to concentrate light into the outer segment. This occurs regardless of photoreceptor structure (fig. 2) and has been shown previously for pigmented droplets (Ives et al., 1983; Wilby et al., 2015). A potential source for this reduction in enhancement may be due to increased reflectivity from the oil droplet interface for higher values of n_{OD} (Wilby et al., 2015).

2. We observe that receptor geometry can affect the extent to which the oil droplet enhances light capture. Firstly, a shorter outer segment may benefit from greater enhancement (fig. 3). Secondly, simulations confirm the intuition that a larger oil droplet captures light over a larger area and collects more light into the outer segment and so gives greater enhancement (fig. 4). Finally, wider outer segments also benefit from greater enhancement (fig. 4). The root of this observation lies in waveguide phenomena - a wider outer segment will support a greater number waveguide modes (Snyder and Love, 1983; Stavenga, 2003).

3. Geometrical models of photoreceptor sensitivity (Land, 1981; Warrant and Nilsson, 1998) are not designed to take waveguide optics into account. The

normal assumption is that oil droplets focus all light within their cross-sectional areas into the outer segment (eg Lind and Kelber, 2009a). Here, we have seen that this is not the case and when optical effects are incorporated, $F<1$. The implication is that calculated absolute sensitivities of photoreceptors with oil droplets will be reduced if optical effects are included.

One factor that may hinder the ability of oil droplets to enhance light capture is their position relative to the outer segment; oil droplets are in direct contact with the outer segment aperture. Man-made ball lens-waveguide assemblies are an equivalent synthetic system used to couple light from light sources into dielectric waveguides. Here, the highest coupling efficiencies in these systems are seen for intermediate distances between ball lens and waveguide entrance (Ratowsky et al., 1997) and although operating on a larger scale, similar optical considerations apply.

The curves in figs. 2-4 are non-trivial functions of wavelength, displaying local minima and varying behaviour depending upon the photoreceptor structure. This is due to the relative prominence of the influence of contributing optical phenomena including Mie scattering and waveguidance, which have contrasting wavelength dependencies. For instance, the wavelength position of peaks and troughs in the enhancement factor curves correspond with Mie scattering behaviour such as that predicted by the anomalous diffraction approximation (van de Hulst, 1981). Differing combinations of refractive index and oil droplet diameter result in a Mie scattering efficiency curve that oscillates as a function of wavelength at the length scales seen here. In contrast, power contained in a dielectric waveguide decreases gradually with increasing wavelength (Snyder and Love, 1983). Both of these phenomena play a role in governing the sensitivity of oil droplet-bearing photoreceptors. By using FDTD simulation, a full-wave optical approach, all classical optical effects are included in the solution of Maxwell's equations.

Pigmented oil droplets

None of the pigmented droplets examined here increased light capture around the peak absorbance of the visual pigment (fig. 7). This tells a very different story to the general assumption that all light within the inner segment is focused by the oil droplet into the outer segment. It is only the transparent oil droplets that consistently exhibit

the increased enhancement factors. The ellipsoid does seem to generally increase the enhancement factors, particularly in the VS cones of *G. gallus* which, in the presence of the ellipsoid, increases light capture by 50%. This essentially justifies the retention of transparent oil droplets in VS/UVS cones, meaning that they improve signal-to-noise ratio in these cones. Pigmented droplets, separately, tune spectral sensitivity in the other cone types, but do not help with light capture. This effect of the ellipsoid increasing on-axis transmission of light into the outer segment is consistent with earlier observations (Govardovskii et al., 1981; Wilby et al., 2015).

Absolute sensitivity

The prediction from the calculations presented here is that oil droplets do not collect as much light as geometrical calculations would predict. Therefore, the expectation is that oil droplet-bearing cones are not as sensitive to light as previously thought. However, this is not a straightforward prediction to test. In a recent experiment, Olsson et al. (2017) performed behavioural tests of the intensity thresholds in a colour discrimination task in chickens. Discriminability was modelled using the receptor noise limited model in which cone quantum catches were calculated using both geometrical considerations and the optical simulation approach presented here. The optical simulation sensitivity models that incorporated wave-optical effects predicted the number of photoreceptors required an order of magnitude more accurately than those relying on geometrical calculations. This demonstrates, to some extent, that wave-optical phenomena in oil droplet-bearing cones do indeed impact absolute sensitivity of photoreceptors.

Further, absolute sensitivity is also governed by the angular sensitivity of a photoreceptor (as well as the *f*-number of the eye). Here, we have concentrated on light propagating parallel to the photoreceptor axis, whereas previous studies have observed the effect of certain oil droplets on the angular sensitivity of cone photoreceptors (Govardovskii et al., 1981; Wilby et al., 2015). Both studies found that oil droplets narrow the angular sensitivity, Govardovskii et al. explain that though the oil droplet increases the quantum catch for on-axis propagation of light, due to the narrowing of angular sensitivity, it results in no overall greater sensitivity.

Outer segments in enhancement calculations

Ives at al. (1983) reported enhancement factors in the cone of the turtle (*T. scripta elegans*) of 2-4 for the clear, yellow and red oil droplets corresponding to the SWS, MWS and LWS cones respectively. However, in our calculations, we find no enhancement factors >2 for any of the experimentally valid properties used in our calculations. Importantly, the calculations of Ives at al. (1983), only used an analytical Mie scattering approach, and therefore by definition were not to include the optical properties and structure of the outer segment itself in their models. In an attempt to reconcile the differences between these two sets of calculations, we performed simulations using similar properties to those used in Ives et al. (1983) with and without the outer segment. Our results (see Supplementary fig. S3) show that without the outer segment (ie the oil droplet is isolated in isotropic material of a single refractive index) enhancement factors appear to greatly exceed 2 at wavelengths where there is little absorption in the oil droplet. Overall, our results show that it is essential to include both the outer segment and ellipsoid in any optical model of photoreceptors

Optics and spectral sensitivity

One noticeable effect is that the enhancement factor is wavelength-dependent. This perhaps leads to modulation of the receptor sensitivity via the alteration of the relative abundance of photons of certain wavelengths within the outer segment. It has been previously shown that real photoreceptor spectral sensitivity is altered by waveguide effects. Due to the wavelength dependency of guided power, there is greater sensitivity to shorter wavelengths in the photoreceptors of the Small White butterfly (Stavenga and Arikawa, 2011). It remains to be seen whether scattering effects such as those investigated here alter the relative spectral sensitivity of vertebrate photoreceptors with any measurable significance. Models of spectral sensitivity that only include absorption have been relatively accurate so far in explaining colour vision, in birds for instance (Vorobyev and Osorio, 1998).

Evolutionary loss of oil droplets

Throughout vertebrate evolution it is unclear whether oil droplets first appeared in the transparent or pigmented form, moreover they may also have switched between states more than once. It also seems that because oil droplets have been lost from various

major lineages, they are not always advantageous (Robinson, 1994; Rowe, 2000; Jacobs and Rowe, 2004). Oil droplets do not seem capable of both improving light capture and tuning spectral sensitivity by filtering at the same time. Under the previous dogma that all oil droplets improve light capture in cones, there seems to be little disadvantage to their presence in the retina. However, we see here that oil droplets must be relatively large and transparent in order to substantially improve light capture. On increasing the size of the oil droplet, fewer receptors can be packed into a certain area of the retina, thus reducing spatial acuity. The transparent oil droplet is essentially a device to improve the signal-to-noise ratio of the cone mechanism and therefore this does come at the expense of visual acuity to a certain extent. We suggest that if a better tool for improving signal-to-noise ratio were evolved which did not sacrifice acuity, that this would be grounds to abandon the transparent oil droplet. Such a feature might be represented by a less noisy visual pigment or perhaps a dynamic spatial pooling mechanism.

Conclusions

We find that optical enhancement provided by oil droplets is highly variable with receptor morphology and refractive index as well as wavelength. Our primary conclusion is that oil droplets almost never collect as much light as predicted by purely geometrical considerations. In general, transparent oil droplets increase the light collected into the outer segment and pigmented droplets decrease for wavelengths around the maximal visual pigment sensitivity. Ellipsoids in avian cones act to alleviate the light loss, resulting in an overall gain in light capture in the VS cone. The ultimate implication for vision in oil droplet-bearing cones is that absolute receptor sensitivity is largely reduced in comparison to models that do not include optical phenomena.

Ethical approval: All applicable international, national, and/or institutional guidelines for the care and use of animals were followed.

Competing interests: No competing interests declared.

Acknowledgements

The authors would like to thank Stephen Soffe for the kind donation of *Xenopus laevis* specimens; Olle Lind for useful discussions, comments on the manuscript and for figure 1; Peter Olsson and Almut Kelber for comments on the manuscript. Chicken silhouette image was designed by freepik. Xenopus and turtle silhouettes modified from photographs by Brian Gratwicke and Jim Capaldi made available on flickr under Creative Commons attribution licenses.

Funding: This work was supported in part by Human Frontiers Science Program (RGP0017/2011 to NWR). DW was funded by EPSRC via the Bristol Center for Functional Nanomaterials (EP/G036780/1) and by the Leverhulme Trust (RPG-2014-363 to NWR).

Author contributions: DW and NWR conceived the study and wrote the paper. DW performed measurements, calculations and analyses.

References

Born, E. and Wolf, M. (1999) *Principles of Optics*: *Electromagnetic theory of propagation, interference and diffraction of light (7th ed.)*. pp. 100-102. Cambridge, UK: Cambridge University Press. doi: 10.1017/CBO9781139644181

Bowmaker, J.K., Heath, L.A., Wilkie, S.E., Hunt, D.M. (1997) Visual Pigments and Oil Droplets from Six Classes of Photoreceptor in the Retinas of Birds. *Vision Res.* **37**, 2183-2194. doi: 10.1016/S0042-6989(97)00026-6

Enoch, J.M. and Tobey Jr., F.L. (1978) Use of the waveguide parameter *V* to determine the difference in the index of refraction between the rat rod outer segment and the interstitial matrix. *J. Opt. Soc. Am.* **68**, 1130-1134. doi:10.1364/JOSA.68.001130

Govardovskiì, V.I., Golovanevskiì, E.I., Zuevam L.V. and Vasil'eva I.L. (1981) Role of cellular organoids in photoreceptor optics (studies on microwave models). *Zh. Evol. Biokhim. Fiziol.* **17**, 492-497 (in Russian).

Hart, N.S. (2001) The Visual Ecology of Avian Cone Photoreceptors. *Prog. Retin. Eye. Res.* **20**, 675-703. doi:10.1016/S1350-9462(01)00009-X

Ives, J.T., Normann, R.A. and Barber, P.W. (1983) Light intensification by cone oil droplets: electromagnetic considerations. *J. Opt. Soc. Am. A* **73**, 1725-1731. doi:10.1364/JOSA.73.001725

Jacobs, G.H. and Rowe, M.P. (2004) Evolution of vertebrate colour vision. *Clin. Exp. Optometry*. **87**, 206-216. doi: 10.1111/j.1444-0938.2004.tb05050.x

Johnston, D. and Hudson, R.A. (1976) Isolation and composition of the carotenoid-containing oil droplets from cone photoreceptors. *Biochim. Biophys. Acta* **424**, 235-245. doi:10.1016/0005-2760(76)90191-0

Land, M.F. (1981) Optics and vision in invertebrates. In *Handbook of Sensory Physiology* vol. VII/6B (Ed. H. Autrum) pp.471-592. Berlin: Springer.

Leertouwer, H.L., Wilts, B.D. and Stavenga, D.G. (2011) Refractive index and dispersion of butterfly chitin and bird keratin measured by polarizing interference microscopy. *Opt. Expr.* **19**, 24061-24066. doi: 10.1364/OE.19.024061

Liebman, P.A. and Granda, A. (1971) Microspectrophotometric measurements of visual pigments in two species of turtle, *Pseudemys scripta* and *Chelonia mydas*. *Vision Res.* **11**, 105–114. doi:10.1016/0042-6989(71)90227-6

Lind, O. and Kelber, A. (2009a) The intensity threshold of colour vision in two species of parrot. *J. Exp. Biol.* **212**, 3693-3699. doi: 10.1242/jeb.035477

Lind, O. and Kelber, A. (2009b) Avian colour vision: effects of variation in receptor sensitivity and noise data on model predictions as compared to behavioural results. *Vision Res.* **49**, 1939-1947. doi: 10.1016/j.visres.2009.05.003

Meyer, A. and Zardoya, R. (2003) Recent advances in the (molecular) phylogeny of vertebrates. *Annu. Rev. Evol. Syst.* **34**, 311-338. doi: 10.1146/annurev.ecolsys.34.011802.132351

Olsson, P., Wilby, D. and Kelber, A. (2017) Spatial summation improves bird color vision in low light intensities. *Vision Res.* **130**, 1-8. doi: 10.1016/j.visres.2016.10.009

Oskooi, A.F., Roundy, D., Ibanescu, M., Bermel, P., Joannopoulos, J.D. and Johnson, S.G. (2010) MEEP: A flexible free-software package for electromagnetic simulations by the FDTD method. *Comp. Phys. Comms.* **181**, 687-702. doi:10.1016/j.cpc.2009.11.008

Ratowsky, R.P., Yang, L., Deri, R.J., Chang, K.W., Kallman, J.S. and Trott, G. (1997) Laser diode to single-mode fiber ball lens coupling efficiency: full-wave calculation and measurements. *Appl. Opt.* **36**, 3435-3438. doi: 10.1364/AO.36.003435

Roberts, N.W., Chiou,, T.-H., Marshall, N.J. and Cronin, T.W. (2009) A biological quarter-wave retarder with excellent achromaticity in the visible wavelength region. *Nat. Photon.* **3**, 641-644. doi:10.1038/nphoton.2009.189

Robinson, S.R. (1994) Early vertebrate colour vision. *Nature* **367**, 121. doi: 10.1038/367121a0

Röhlich, P. and Szél, A. (2000) Photoreceptor cells in the *Xenopus* retina. *Microsc. Res. Tech.* **50**, 327-337. doi: 10.1002/1097-0029(20000901)50:5<327::AID-JEMT2>3.0.CO;2-P

Rowe, M.P. (2000) Inferring the retinal anatomy and visual capabilities of extinct vertebrates. *Palaentologica Electronica* **3**, 1-43.

Schürmann, M., Scholze, J., Müller, P., Chan, C.J., Ekpenyong, A.E., Chalut, K.J. and Guck, J. (2015) *Refractive index measurements of single, spherical cells using digital holographic microscopy*. In: Biophysical Methods in Cell Biology Vol. 125 (ed. E.K. Paluch), pp. 143-159. doi:10.1016/bs.mcb.2014.10.016

Snyder, A.W. and Love, J.D. (1983) Optical Waveguide Theory. Chapman and Hall, London.

Stavenga, D.G. and van Barneveld, H.H. (1975) On dispersion in visual photoreceptors. *Vision Res.* **15**, 1091-1095. doi:10.1016/0042-6989(75)90006-1

Stavenga, D.G. (2003) Angular and spectral sensitivity of fly photoreceptors. I. Integrated facet lens and rhabdomere optics. *J. Comp. Physiol. A* **189**, 1-17. doi: 10.1007/s00359-002-0370-2

Stavenga, D.G. and Arikawa, K. (2011) Photoreceptor spectral sensitivities of the Small White butterfly *Pieris rapae crucivora* interpreted with optical modeling. *J. Comp. Physiol. A* **197**, 373-385. doi: 10.1007/s00359-010-0622-5

Stavenga, D.G. and Wilts, B.D. (2014) Oil droplets of bird eyes: microlenses acting as spectral filters. *Phil. Trans. R. Soc. B* **369**, 20130041. doi:10.1098/rstb.2013.0041

Strother, G.K. (1963) Absorption spectra of retinal oil globules in turkey, turtle and pigeon. *Exp. Cell. Res.* **29**, 349-355. doi: 10.1016/0014-4827(63)90389-6

Toomey, M.B., Collins, A.M., Frederiksen, R., Cornwall, M.C., Timlin, J.A. and Corbo, J.C. (2015) A complex carotenoid palette tunes avian colour vision. *J. R. Soc. Interface* **12**, 20150563. doi:10.1098/rsif.2015.0563

Vorobyev, M. and Osorio, D. (1998) Receptor noise as a determinant of colour thresholds. *Proc, R. Soc. B* **265**, 351-358. doi: 10.1098/rspb.1998.0302.

Vorobyev, M. (2003) Coloured oil droplets enhance colour discrimination. *Proc. R. Soc. B* **270**, 1255-1261. doi:10.1098/rspb.2003.2381

Walls, G.L. (1942) The Vertebrate Eye and its Adaptive Radiation. Hafner, New York.

Warrant, E.J. and Nilsson, D.-E. (1998) Absorption of white light in photoreceptors. *Vision Res.* **38**, 195-207. doi: 10.1016/S0042-6989(97)00151-X

van de Hulst, H.C. (1981) Light scattering by small particles. 2nd Ed., Dover Publications, New York.

Wilby, D., Toomey, M.B., Olsson, P., Frederiksen, R., Cornwall, M.C., Oulton, R., Kelber, A., Corbo, J.C. and Roberts, N.W.. (2015) Optics of cone photoreceptors in the chicken (*Gallus gallus domesticus*) *J. R. Soc. Interface* **12**, 20150591. doi:10.1098/rsif.2015.0591

Young, S.R. and Martin, G.R. (1984) Optics of retinal oil droplets. *Vision Res.* **24**, 129-137. doi:10.1016/0042-6989(84)90098-1

Figures

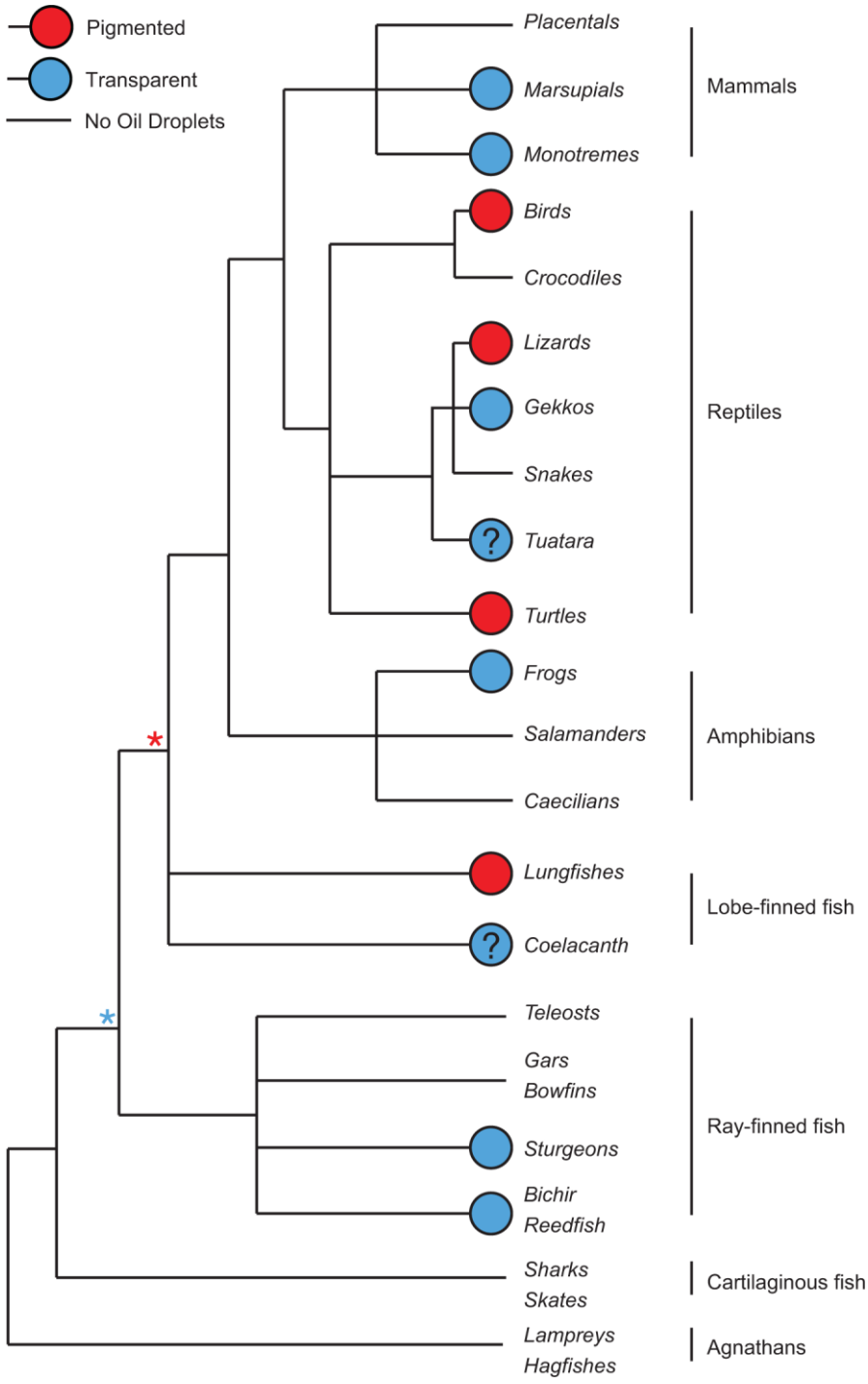

Fig. 1: Summary tree of the pigmentation properties and presence/absence of oil droplets in extant vertebrates. Blue circles indicate that there are no pigmented oil droplets in any cone of a taxon, where red circles show taxa that have at least some

Journal of Experimental Biology • Advance article

pigmented droplets and some transparent, most regularly in the VS and UVS cones. Asterisks indicate the possible first appearance of pigmented or transparent oil droplets. Question marks indicate uncertainties. Source references for oil droplet traits and more detailed notes are provided in the supplementary information (table S1). Tree informed by Meyer and Zardoya (2003). Figure courtesy of Olle Lind.

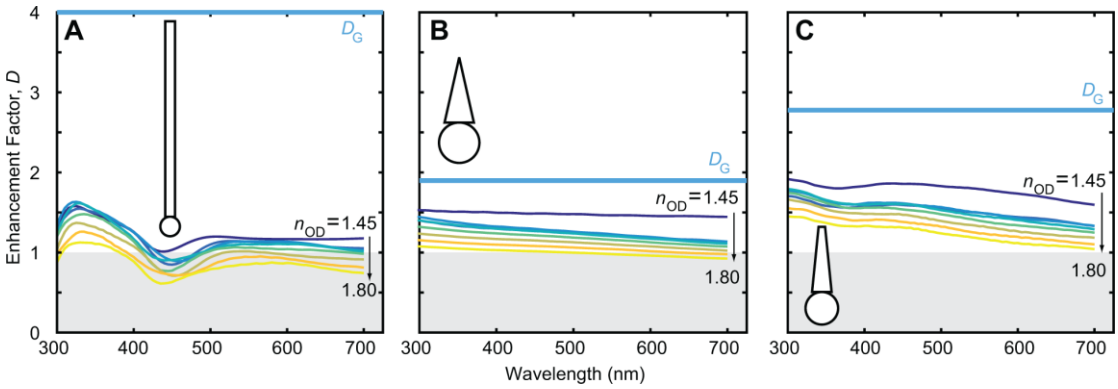

Fig. 2: **Simulated enhancement factor curves for three model photoreceptors.** Based on the dimensions of cones in a) birds (l_{OS}=30 µm, d_{OS}=1.5 µm, d_{OD}=3 µm); b) frogs (l_{OS}=12 µm, tapering d_{OS}=4.5-0 µm, d_{OD}=6.2 µm); and turtles (l_{OS}=10 µm, tapering d_{OS}=3-1 µm, d_{OD}=5 µm). Families of curves were calculated for a wavelength-invariant value of n_{OD} increasing in steps of 0.05 from 1.45-1.8. Grey regions show enhancement factors <1, corresponding to loss of light due to the oil droplet. Thick light blue lines show D_G. In all three cases, the higher the refractive index of the oil droplet, the lower the enhancement factor. In no case did the enhancement factor approach D_G.

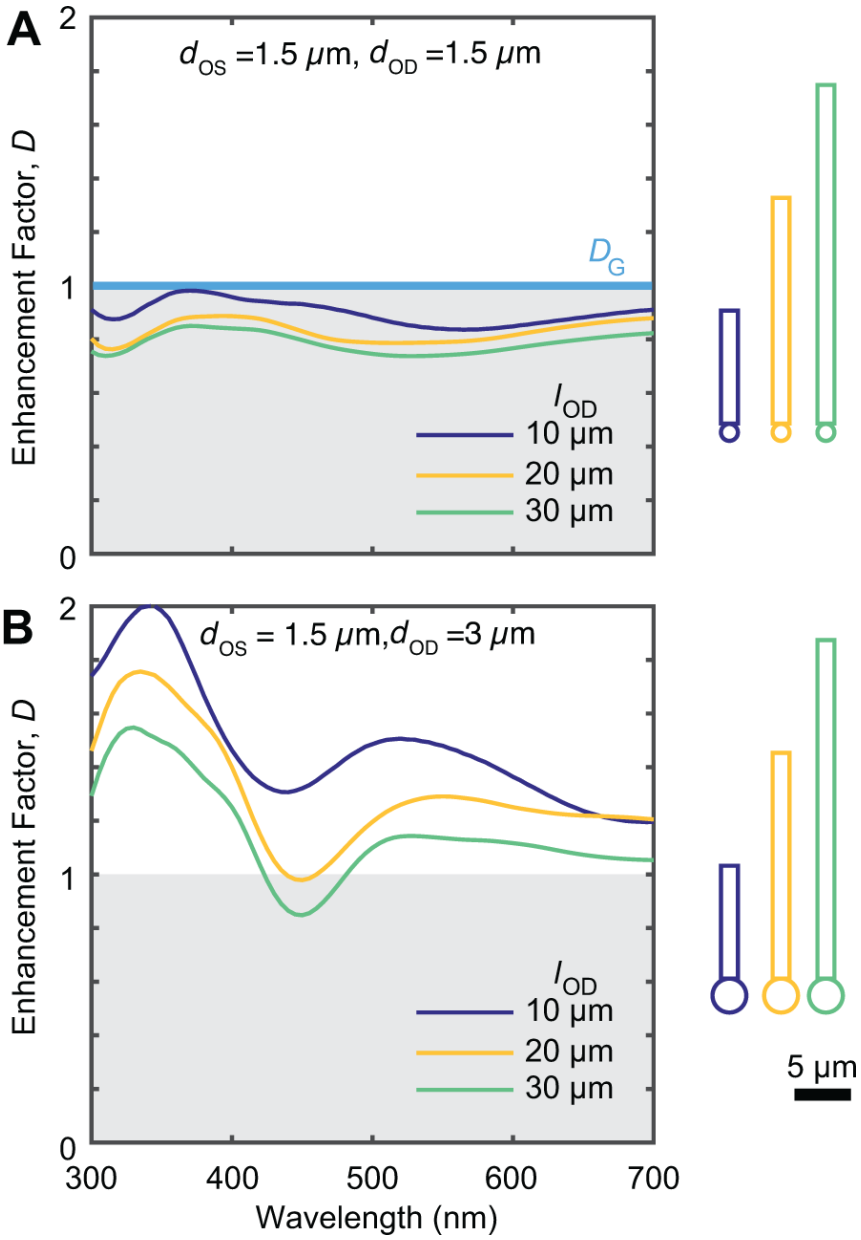

Fig. 3: **Simulated enhancement factors for increasing outer segment length, *l*os.** d_{OS}=1.5 μm and n_{OD}=1.5. Grey regions indicate oil droplets resulting in loss of light. a) d_{OD}=1.5 μm. b) d_{OD}=3 μm. Thick light blue line indicates D_G of 1 in a); D_G = 4 in b), falling outside axis limits. Enhancement is greater for shorter l_{OS} for both values of d_{OD}.

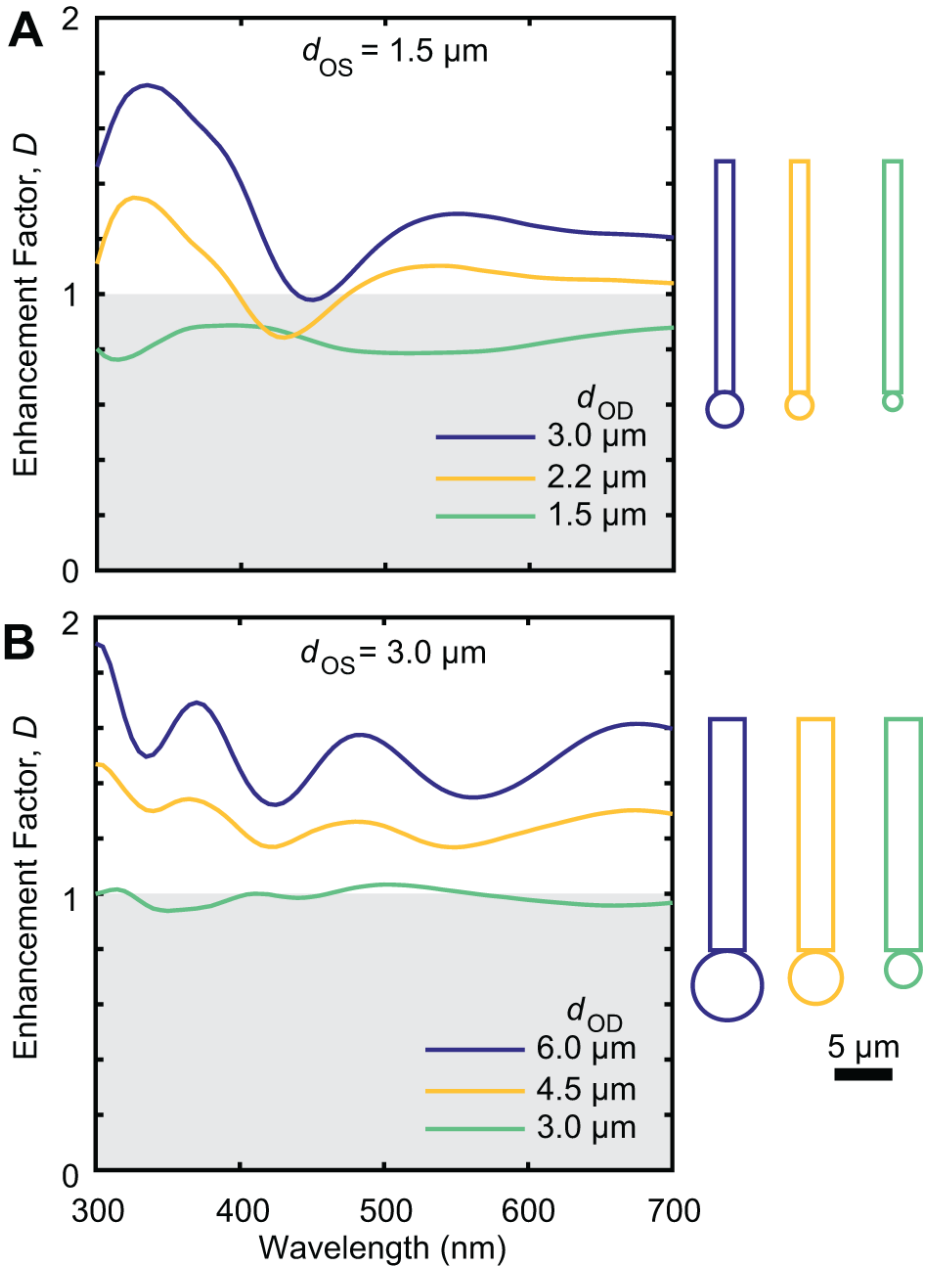

Fig. 4: **Simulated enhancement factors for increasing sizes of oil droplet.** l_{OS}=30 µm and n_{OD}=1.5. Grey regions indicate oil droplets resulting in loss of light. Larger oil droplets result in greater enhancement factors. Wider outer segments and larger oil droplets give larger enhancement factors.

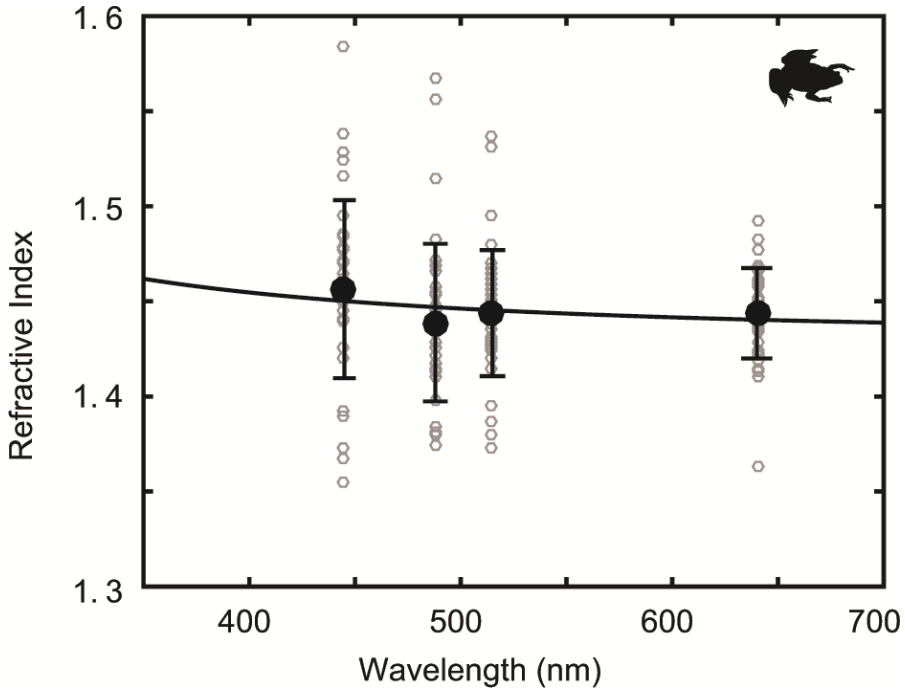

Fig. 5: **Refractive index of *Xenopus laevis* oil droplets measured by digital holographic microscopy.** Grey open circles show individual measurements. Black filled circles show mean values at each wavelength with error bars showing single standard deviations. Line shows Cauchy relation fit to the data points.

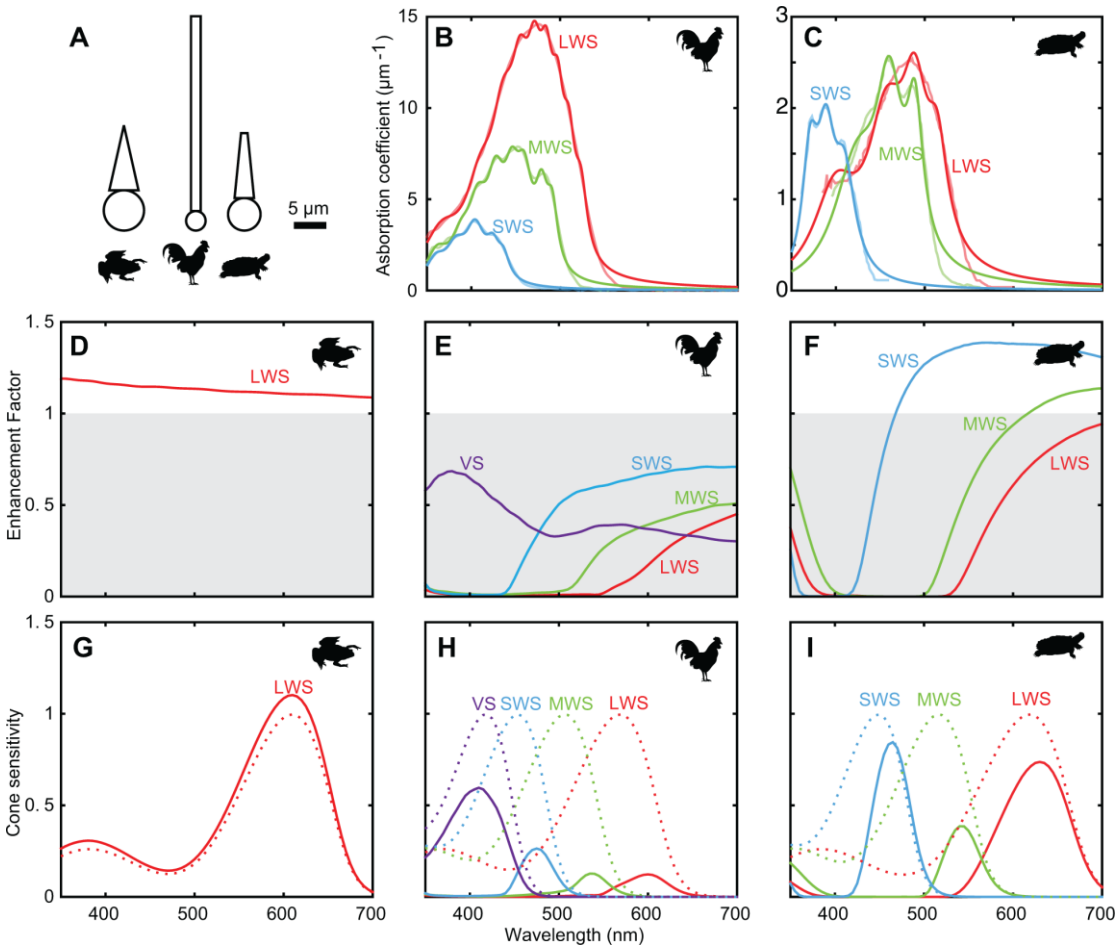

Fig. 6: **Influence of pigmented and unpigmented oil droplets on sensitivity of cones in *Xenopus laevis*, *Gallus gallus* and *Trachemys scripta elegans* in the absence of the ellipsoid.** a) Relative cone photoreceptor dimensions used in calculations. b) and c) Absorption coefficients of the LWS, MWS and SWS cone oil droplets in the chicken and turtle respectively. Pale lines show measured spectra, dark lines show modelled spectra. d)-f) Oil droplet enhancement factors for the cone photoreceptors of the three species. g)-i) Relative cone sensitivities using the calculated enhancement factors. Dotted lines show the visual pigment absorbance templates. Solid lines show the result of multiplying the normalized visual pigment absorbance by the enhancement factor. d) and g) *Xenopus laevis*. b), e) and h) *Gallus gallus*. c), f) and i) *Trachemys scripta elegans*.

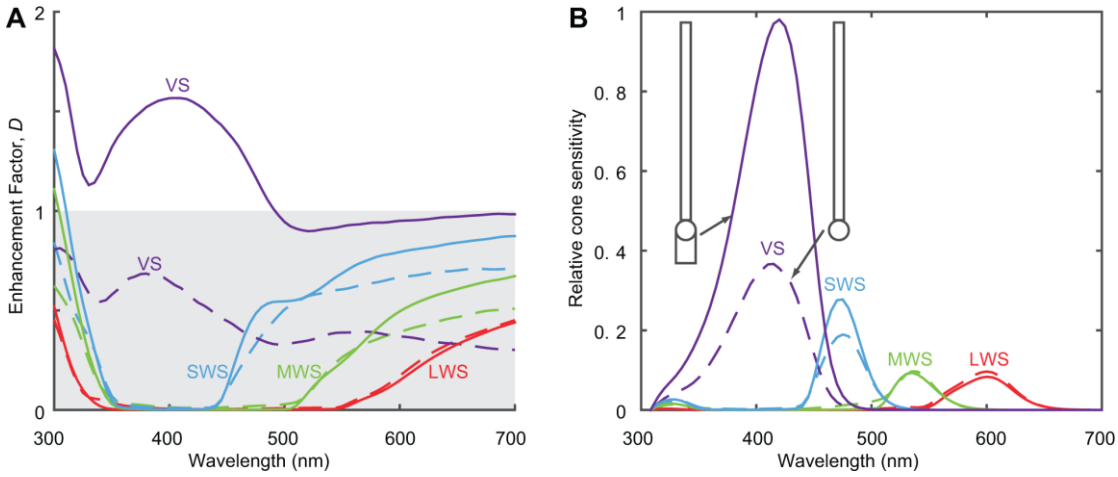

Fig. 7: Impact of the ellipsoid on enhancement factor and relative sensitivity for chicken cone photoreceptors. a) Enhancement factors with and without the ellipsoid. Dashed lines show enhancement factors without the ellipsoid; solid lines show enhancement factors including both ellipsoid and oil droplet. Greatest increase is seen for the VS cone, which with the addition of an ellipsoid has an enhancement factor much larger than 1. In the SWS and MWS receptors, a small increase is seen. In the LWS receptor, a very slight decrease in enhancement is seen for the visible spectrum. b) Relative sensitivity of chicken cones with and without the ellipsoid. Ocular media transmittance is included as measured by Lind and Kelber (2009b).

Supplementary information

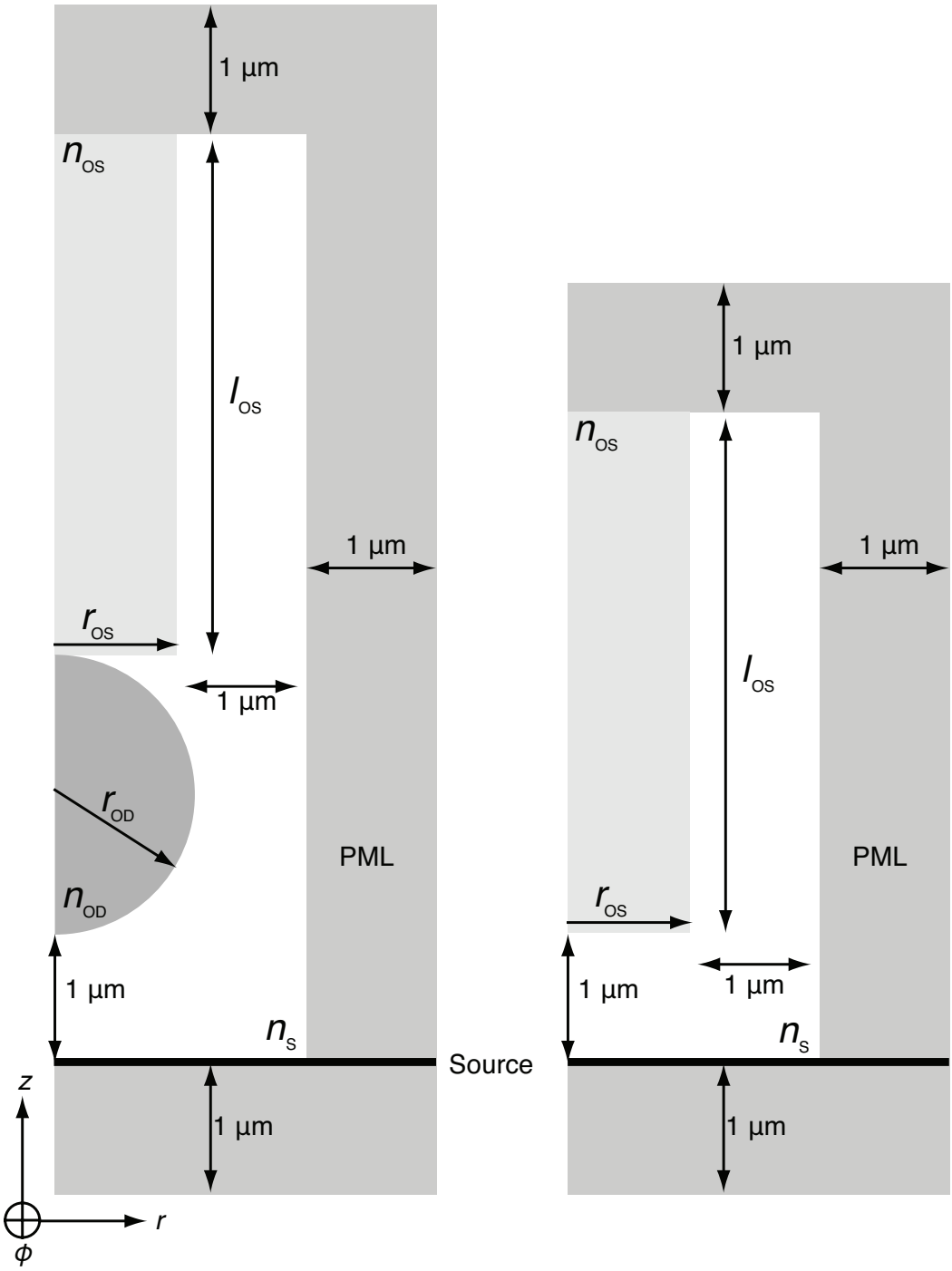

Fig S1: Example schematics of the simulation environment. Thick black line indicates the plane wave source. Calculations are performed in cylindrical polar coordinates (r, φ, z). φ-direction is normal to the plane of the page here. Simulation is surrounded on three sides with perfectly-matched layers (PML) which prevent numerical reflections from the sides of the simulation environment (Oskooi et al. 2010).

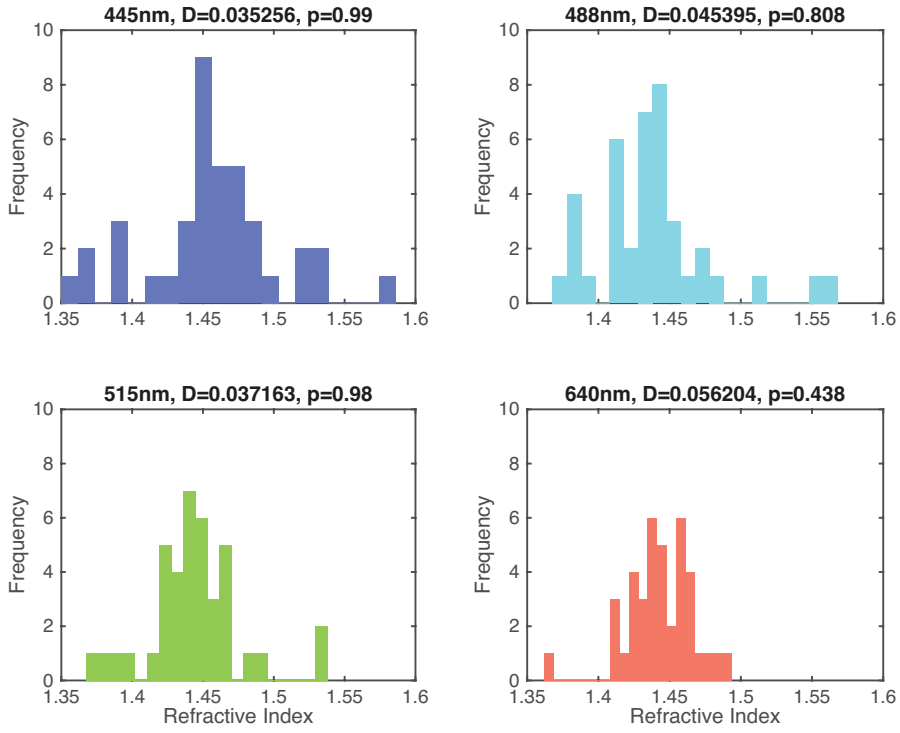

Fig S2: Histograms of the refractive indices of *Xenopus* oil droplets as measured at four wavelengths. *D* values show the result of Hartigans' dip test, which tests for multimodality in a distribution. None of these distributions demonstrate significant multimodality, indicating that in terms of refractive index, all *Xenopus* oil droplets measured are from the same population (ie there is not more than one type of oil droplet with respect to refractive index).

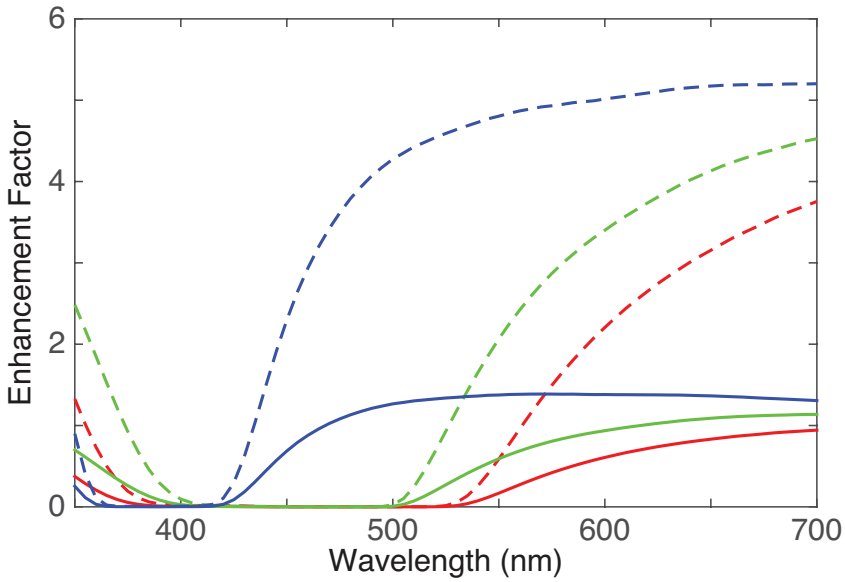

Fig S3: Calculations of enhancement with and without outer segments as a comparison to the Mie scattering calculations of Ives et al. (1983) for the receptor geometry, refractive indices and oil droplet absorption spectra of the turtle *Trachemys scripta elegans*. Solid lines show enhancement factors including the outer segment and dashed lines show calculations without. When the outer segment is not present we recover greater enhancement factors that approach those calculated by Ives et al. (1983). This is due to the waveguiding effect of the outer segment, which allows it to confine light to its volume even without the presence of the oil droplet. Red lines – LWS cone. Green lines – MWS cone. Blue lines – SWS cone.

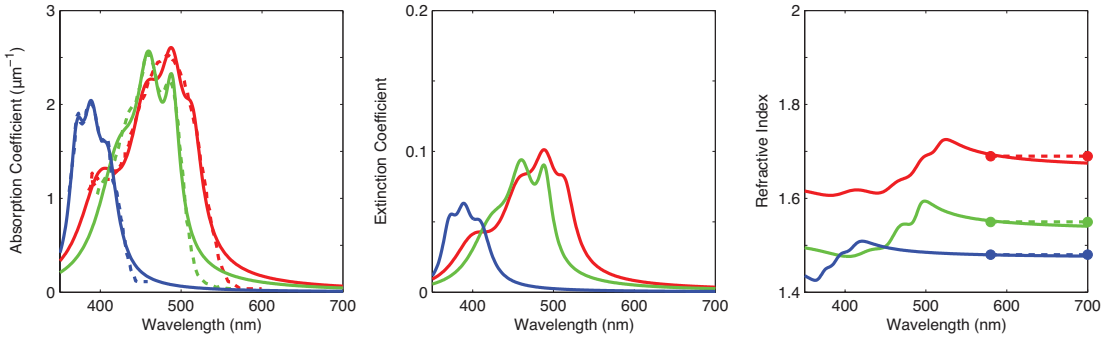

Fig. S4: Absorption coefficients and optical properties of the oil droplets of *T. scripta elegans*. Absorption coefficient modelled using the methods of Wilby et al. (2015). Solid lines show model spectra. Dotted lines show spectra from Strother (1963) and Liebman & Granda (1971). Calculated extinction coefficient and real refractive index. Circles show refractive index values from Ives et al. (1983) and the spectral range over which these were measured. Red lines – LWS cone. Green lines – MWS cone. Blue lines – SWS cone.

Table S1 can be found in a separate excel file.

Click here to Download Table S1

Table S2: Dimensions and refractive indices used in simulations of chicken, turtle and *Xenopus* photoreceptors.

Chicken	**Value**	**Source**
Oil droplet diameter	3.0 µm	Wilby et al. (2015)
Oil droplet refractive index	See Wilby et al. (2015) for details	
Ellipsoid length	3.5 µm	Wilby et al. (2015)
Ellipsoid diameter	3.0 µm	Wilby et al. (2015)
Ellipsoid refractive index	1.43	Wilby et al. (2015)
Outer segment diameter	1.5 µm	Wilby et al. (2015)
Outer segment length	30 µm	Wilby et al. (2015)
Outer segment refractive index	1.45	Wilby et al. (2015)

Turtle	**Value**	**Source**
Oil droplet diameter	5.0 µm	Ives et al. (1983)
Oil droplet refractive index	Refractive index from Ives et al. (1983). Pigment absorption from Strother (1963); Liebman & Granda (1971). See fig. S4.	
Outer segment base diameter	3.0 µm	Ives et al. (1983)
Outer segment end diameter	0.5 µm	Ives et al. (1983)
Outer segment length	10 µm	Ives et al. (1983)
Outer segment refractive index	1.45	Wilby et al. (2015)

Xenopus	**Value**	**Source**
Oil droplet diameter	6.2 µm	Röhlich & Szél (2000)
Oil droplet refractive index	See fig. 4 (main text)	Present study
Outer segment base diameter	4.5 µm	Röhlich & Szél (2000)
Outer segment end diameter	0 µm	Röhlich & Szél (2000)
Outer segment length	12 µm	Röhlich & Szél (2000)
Outer segment refractive index	1.45	Wilby et al. (2015)

References

Ives, J.T., Normann, R.A. and Barber, P.W. (1983) Light intensification by cone oil droplets: electromagnetic considerations. *J. Opt. Soc. Am. A* **73**, 1725-1731. doi:10.1364/JOSA.73.001725

Liebman, P.A. and Granda, A. (1971) Microspectrophotometric measurements of visual pigments in two species of turtle, *Pseudemys scripta* and *Chelonia mydas*. *Vision Res.* **11**, 105–114. doi:10.1016/0042-6989(71)90227-6

Oskooi, A.F., Roundy, D., Ibanescu, M., Bermel, P., Joannopoulos, J.D. and Johnson, S.G. (2010) MEEP: A flexible free-software package for electromagnetic simulations by the FDTD method. *Comp. Phys. Comms.* **181**, 687-702. doi:10.1016/j.cpc.2009.11.008

Röhlich, P. and Szél, A. (2000) Photoreceptor Cells in the *Xenopus* Retina. *Microsc. Res. Tech.* **50**(5):327-337. doi: 10.1002/1097-0029(20000901)50:5<327::AID-JEMT2>3.0.CO;2-P

Strother, G.K. (1963) Absorption spectra of retinal oil globules in turkey, turtle and pigeon. *Exp. Cell. Res.* **29**, 349-355. doi: 10.1016/0014-4827(63)90389-6

Wilby, D., Toomey, M.B., Olsson, P., Frederiksen, R., Cornwall, M.C., Oulton, R., Kelber, A., Corbo, J.C. and Roberts, N.W. (2015) Optics of cone photoreceptors in the chicken (*Gallus gallus domesticus*). *J. R. Soc. Interface* **12**:20150591. doi: 10.1098/rsif.2015.0591

Supplementary information

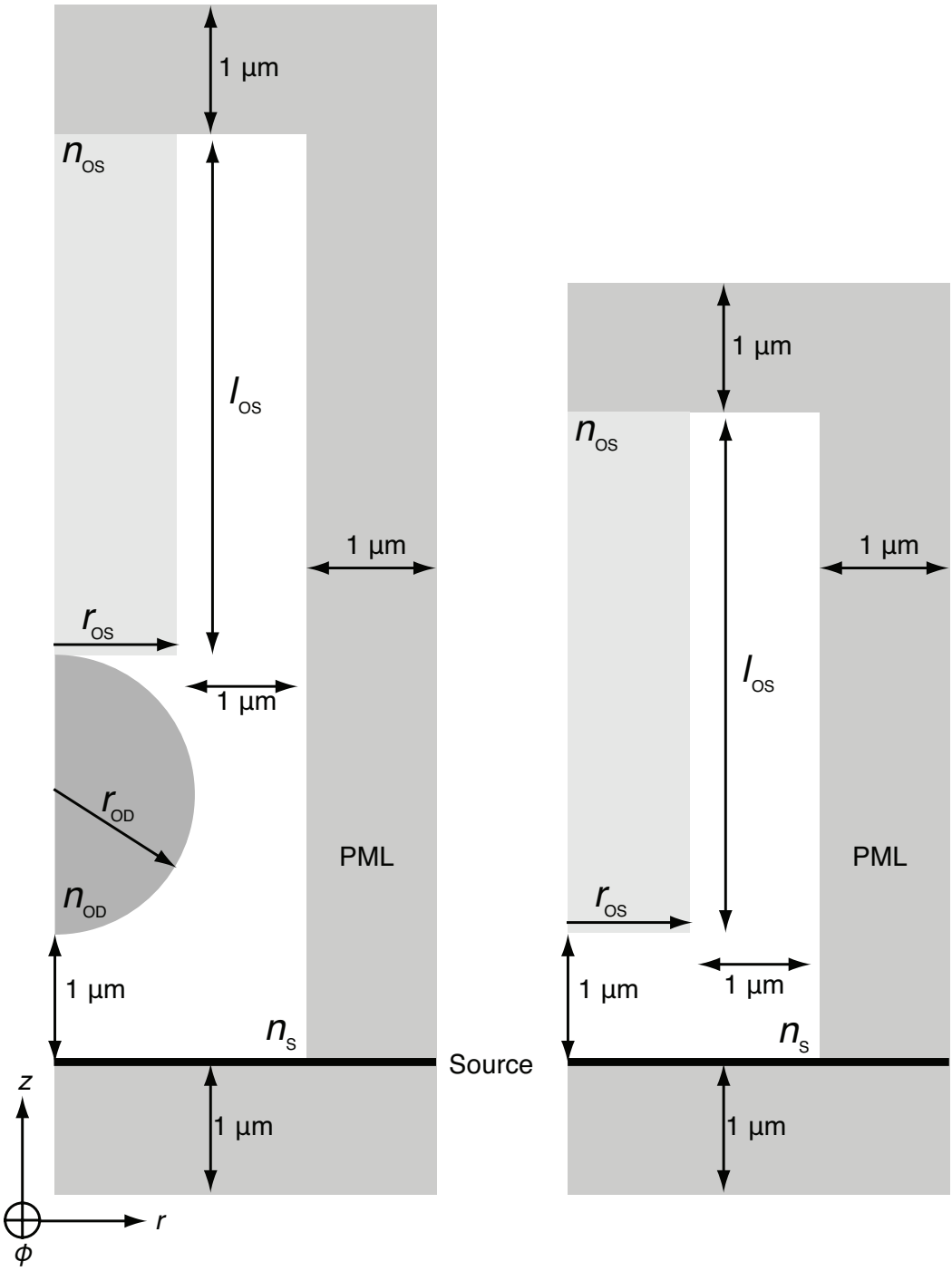

Fig S1: Example schematics of the simulation environment. Thick black line indicates the plane wave source. Calculations are performed in cylindrical polar coordinates (r, φ, z). φ-direction is normal to the plane of the page here. Simulation is surrounded on three sides with perfectly-matched layers (PML) which prevent numerical reflections from the sides of the simulation environment (Oskooi et al. 2010).

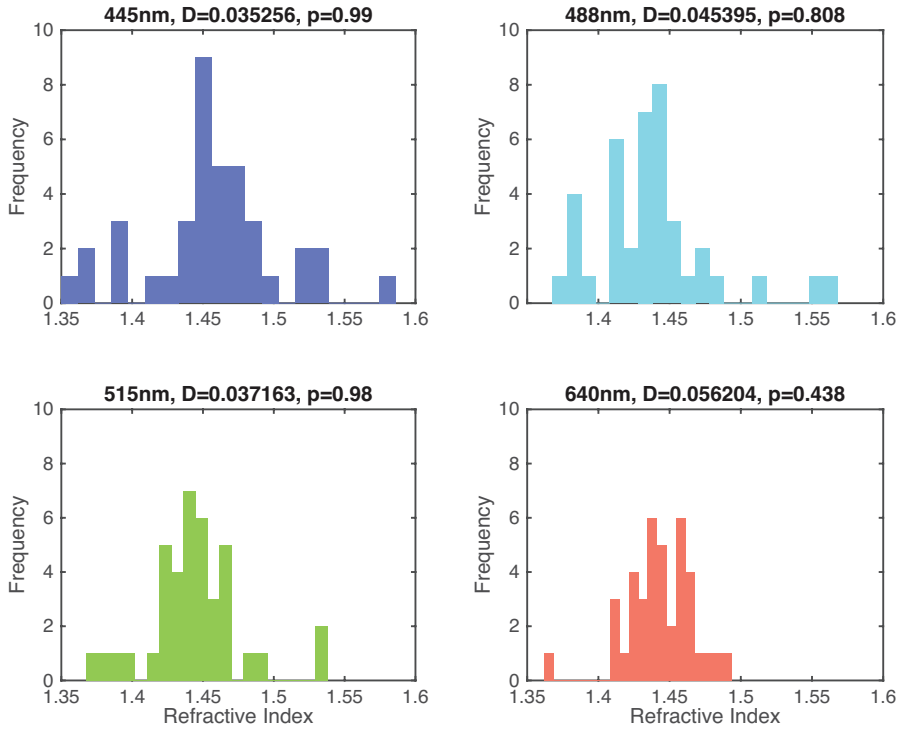

Fig S2: Histograms of the refractive indices of *Xenopus* oil droplets as measured at four wavelengths. *D* values show the result of Hartigans' dip test, which tests for multimodality in a distribution. None of these distributions demonstrate significant multimodality, indicating that in terms of refractive index, all *Xenopus* oil droplets measured are from the same population (ie there is not more than one type of oil droplet with respect to refractive index).

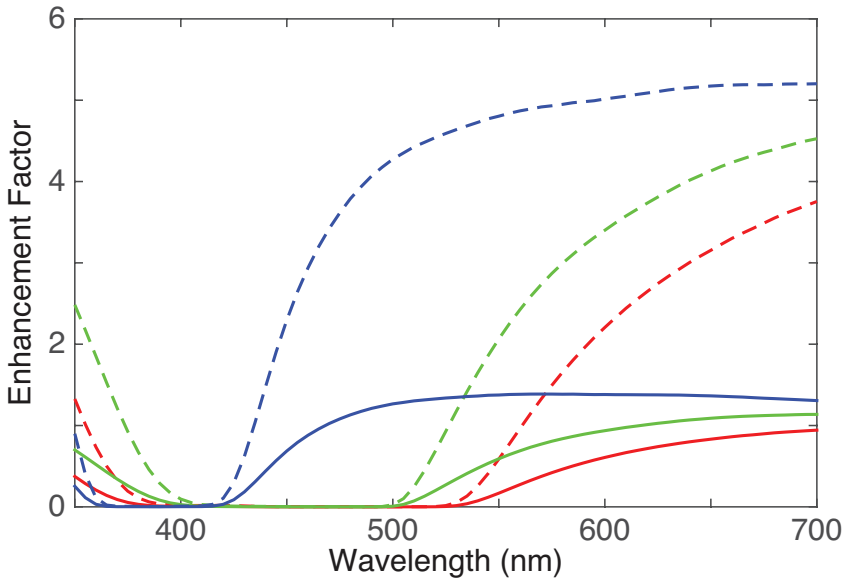

Fig S3: Calculations of enhancement with and without outer segments as a comparison to the Mie scattering calculations of Ives et al. (1983) for the receptor geometry, refractive indices and oil droplet absorption spectra of the turtle *Trachemys scripta elegans*. Solid lines show enhancement factors including the outer segment and dashed lines show calculations without. When the outer segment is not present we recover greater enhancement factors that approach those calculated by Ives et al. (1983). This is due to the waveguiding effect of the outer segment, which allows it to confine light to its volume even without the presence of the oil droplet. Red lines – LWS cone. Green lines – MWS cone. Blue lines – SWS cone.

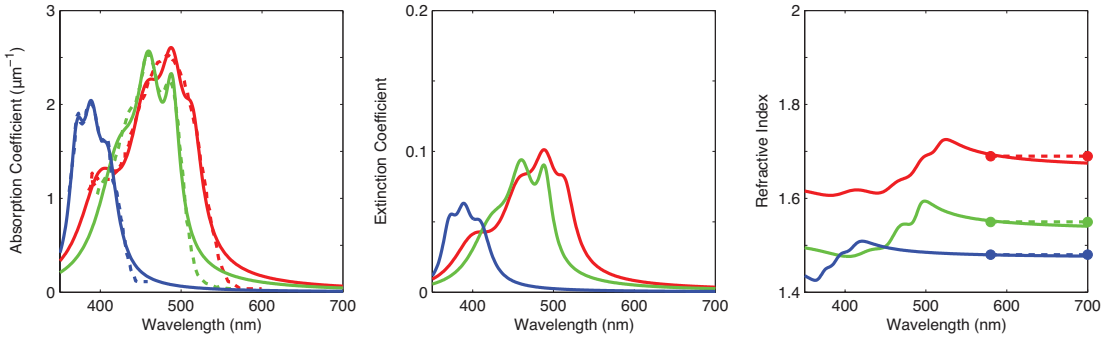

Fig. S4: Absorption coefficients and optical properties of the oil droplets of *T. scripta elegans*. Absorption coefficient modelled using the methods of Wilby et al. (2015). Solid lines show model spectra. Dotted lines show spectra from Strother (1963) and Liebman & Granda (1971). Calculated extinction coefficient and real refractive index. Circles show refractive index values from Ives et al. (1983) and the spectral range over which these were measured. Red lines – LWS cone. Green lines – MWS cone. Blue lines – SWS cone.

Table S1 can be found in a separate excel file.

Click here to Download Table S1

Table S2: Dimensions and refractive indices used in simulations of chicken, turtle and *Xenopus* photoreceptors.

Chicken	**Value**	**Source**
Oil droplet diameter	3.0 µm	Wilby et al. (2015)
Oil droplet refractive index	See Wilby et al. (2015) for details	
Ellipsoid length	3.5 µm	Wilby et al. (2015)
Ellipsoid diameter	3.0 µm	Wilby et al. (2015)
Ellipsoid refractive index	1.43	Wilby et al. (2015)
Outer segment diameter	1.5 µm	Wilby et al. (2015)
Outer segment length	30 µm	Wilby et al. (2015)
Outer segment refractive index	1.45	Wilby et al. (2015)

Turtle	**Value**	**Source**
Oil droplet diameter	5.0 µm	Ives et al. (1983)
Oil droplet refractive index	Refractive index from Ives et al. (1983). Pigment absorption from Strother (1963); Liebman & Granda (1971). See fig. S4.	
Outer segment base diameter	3.0 µm	Ives et al. (1983)
Outer segment end diameter	0.5 µm	Ives et al. (1983)
Outer segment length	10 µm	Ives et al. (1983)
Outer segment refractive index	1.45	Wilby et al. (2015)

Xenopus	**Value**	**Source**
Oil droplet diameter	6.2 µm	Röhlich & Szél (2000)
Oil droplet refractive index	See fig. 4 (main text)	Present study
Outer segment base diameter	4.5 µm	Röhlich & Szél (2000)
Outer segment end diameter	0 µm	Röhlich & Szél (2000)
Outer segment length	12 µm	Röhlich & Szél (2000)
Outer segment refractive index	1.45	Wilby et al. (2015)

References

Ives, J.T., Normann, R.A. and Barber, P.W. (1983) Light intensification by cone oil droplets: electromagnetic considerations. *J. Opt. Soc. Am. A* **73**, 1725-1731. doi:10.1364/JOSA.73.001725

Liebman, P.A. and Granda, A. (1971) Microspectrophotometric measurements of visual pigments in two species of turtle, *Pseudemys scripta* and *Chelonia mydas*. *Vision Res.* **11**, 105–114. doi:10.1016/0042-6989(71)90227-6

Oskooi, A.F., Roundy, D., Ibanescu, M., Bermel, P., Joannopoulos, J.D. and Johnson, S.G. (2010) MEEP: A flexible free-software package for electromagnetic simulations by the FDTD method. *Comp. Phys. Comms.* **181**, 687-702. doi:10.1016/j.cpc.2009.11.008

Röhlich, P. and Szél, A. (2000) Photoreceptor Cells in the *Xenopus* Retina. *Microsc. Res. Tech.* **50**(5):327-337. doi: 10.1002/1097-0029(20000901)50:5<327::AID-JEMT2>3.0.CO;2-P

Strother, G.K. (1963) Absorption spectra of retinal oil globules in turkey, turtle and pigeon. *Exp. Cell. Res.* **29**, 349-355. doi: 10.1016/0014-4827(63)90389-6

Wilby, D., Toomey, M.B., Olsson, P., Frederiksen, R., Cornwall, M.C., Oulton, R., Kelber, A., Corbo, J.C. and Roberts, N.W. (2015) Optics of cone photoreceptors in the chicken (*Gallus gallus domesticus*). *J. R. Soc. Interface* **12**:20150591. doi: 10.1098/rsif.2015.0591